

Large non-Gaussianities with Intermediate Shapes from Quasi-Single Field Inflation

Xingang Chen¹ and Yi Wang²

¹*Center for Theoretical Physics,
Massachusetts Institute of Technology,
Cambridge, MA 02139*

²*Physics Department, McGill University,
Montreal, H3A2T8, Canada*

We study the slow-roll inflation models, where the inflaton slow-rolls along a trajectory whose orthogonal directions are lifted by potentials with masses of order the Hubble parameter. In these models large non-Gaussianities can be generated through the transformation from the isocurvature modes to the curvature mode, once the inflaton trajectory turns. We find large bispectra with one-parameter family of novel shapes, interpolating between the equilateral and local shape. According to the in-in formalism, the shapes of these non-Gaussianities are different from a simple projection from the isocurvature non-Gaussian correlation functions.

Introduction. Inflation [1] is the leading candidate for creating the homogeneous and isotropic universe and generating the primordial density fluctuations for large scale structure. The condition for inflation to happen is that the inflatons slow-roll near the top of the potential for sufficiently long time, so that the vacuum energy drives the accelerated expansion of the Universe.

Generically, it is found that such a condition needs to be finely-tuned, at least for various types of models that have sensible UV completion [2]. For slow-roll inflation, this means that the generic inflaton potential has a steep shape, characterized by a mass of order the Hubble parameter H . On the other hand, it is general that the inflaton can roll in a space with multiple light fields. So at least one of the directions needs to be fine-tuned. A combination of these two aspects suggests a generic situation – the inflaton slow-rolls along a trajectory whose orthogonal directions are lifted by potentials with masses of order H . We call this class of models the quasi-single field inflation. If the inflaton trajectory is straight, this is equivalent to the single field inflation, which generates unobservably small primordial non-Gaussianities [3]. However, as we will show in this paper, once the trajectory turns, large non-Gaussianities with novel shapes can be generated, which are potentially detectable in current and future experiments.

We call the mode in the tangential direction the curvature mode, and the modes in the perpendicular directions the isocurvature modes. The reason that the non-Gaussianities originated from the curvature mode are very small is that the potential is flat. Since the isocurvature modes in our model are massive, $m \sim H$, and can have large higher order interactions, the non-Gaussian correlation functions of the isocurvature modes can be very large. However, in dS space the amplitude of the quantum fluctuations of a massive field decays exponentially after horizon exit, and also fast oscillating if $m \gg H$. This is why such modes are usually not considered. But for $m \sim H$, the suppression due to oscillation

is only marginal. In the mean while, although the isocurvature amplitude still decays, the part of it that is transferred to the tangential direction through turning trajectory becomes part of the curvature mode, which remains constant after horizon exit. The non-Gaussianities in the isocurvature modes are thus transferred in this way. This is the main physical picture behind our calculation.

We use the in-in formalism [4] to compute the precise momentum dependence (shapes) of the bispectra. In this formalism, the natural way to implement the transformation from the isocurvature to curvature mode is to introduce a two-point transfer vertex between the two modes. It is then straightforward to do a perturbative calculation for correlation functions according to the usual Feynman diagrams. As we will see, the effect of the transfer vertex is not a simple projection of the three-point function of the isocurvature modes.

During the computation, we find that two equivalent representations of the in-in formalism, namely the original factorized form and the commutator form, are computationally advantageous in complimentary ways. In certain parameter space, each representation encounters spurious divergence either in IR or UV. These divergences are called spurious because they will eventually be cancelled, but significantly complicate the analytical and numerical calculations. They are completely absent, however, when viewed in a different representation.

We find a one-parameter family of bispectrum shapes, lying in-between the well-known equilateral and local shape. The shape sensitively depends on the mass of the isocurvature mode; the size depends on the turning angular velocity and the cubic interaction strength among isocurvature modes.

The model, mode functions and transfer vertex. We consider a two-field model as an example. It is convenient to write the action in terms of the fields, θ and σ , that are tangential and orthogonal to the turning trajectory,

respectively,

$$S = \int d^4x \sqrt{-g} \left[\frac{1}{2} (R + \sigma)^2 g^{\mu\nu} \partial_\mu \theta \partial_\nu \theta + \frac{1}{2} g^{\mu\nu} \partial_\mu \sigma \partial_\nu \sigma - V_{sr}(\theta) - V(\sigma) \right], \quad (1)$$

where R is the radius of the turning trajectory. The $V_{sr}(\theta)$ is a usual slow-roll potential and we choose the rolling velocity $\dot{\theta}_0 > 0$. The potential

$$V(\sigma) = \frac{1}{2} m_\sigma^2 \sigma^2 + \frac{1}{6} V''' \sigma^3 + \dots \quad (2)$$

traps the σ field at $\sigma = 0$ [5]. In principle, the parameters that characterize the turning trajectory, $\dot{\theta}_0$ and R , and the cubic interaction strength V''' , can vary along the trajectory. In this paper we consider the constant turn case in which they are all constant.

We perform the perturbation in the gauge where the scale factor $a(t)$ is homogeneous. The leading kinematic Hamiltonian density for the quantum fluctuations, $\delta\theta_I$ and $\delta\sigma_I$, in the interaction picture is

$$\begin{aligned} \mathcal{H}_0 = & a^3 \left[\frac{1}{2} R^2 \dot{\delta\theta}_I^2 + \frac{R^2}{2a^2} (\partial_i \delta\theta_I)^2 \right. \\ & \left. + \frac{1}{2} \dot{\delta\sigma}_I^2 + \frac{1}{2a^2} (\partial_i \delta\sigma_I)^2 + \frac{1}{2} (m_\sigma^2 + 7\dot{\theta}_0^2) \delta\sigma_I^2 \right]. \quad (3) \end{aligned}$$

The leading interaction Hamiltonian density is

$$\mathcal{H}_2^I = -c_2 a^3 \delta\sigma_I \dot{\delta\theta}_I, \quad (4)$$

$$\mathcal{H}_3^I = c_3 a^3 \delta\sigma_I^3, \quad (5)$$

where $c_2 = 2R\dot{\theta}_0$, $c_3 = V'''/6$ are constants.

We quantize the fields $\delta\theta_I$ and $\delta\sigma_I$ in the momentum space \mathbf{p} , $\delta\theta_{\mathbf{p}}^I = u_{\mathbf{p}} a_{\mathbf{p}} + u_{-\mathbf{p}}^* a_{-\mathbf{p}}^\dagger$, $\delta\sigma_{\mathbf{p}}^I = v_{\mathbf{p}} b_{\mathbf{p}} + v_{-\mathbf{p}}^* b_{-\mathbf{p}}^\dagger$, where $a_{\mathbf{p}}$ and $b_{\mathbf{p}}$ are independent of each other and each satisfies the usual commutation relation. The mode functions in terms of the conformal time $\tau = \int dt/a(t)$ are

$$u_{\mathbf{p}} = \frac{H}{R\sqrt{2p^3}} (1 + ip\tau) e^{-ip\tau}, \quad (6)$$

$$v_{\mathbf{p}} = -ie^{i(\nu+\frac{1}{2})\frac{\pi}{2}} \frac{\sqrt{\pi}}{2} H(-\tau)^{3/2} H_\nu^{(1)}(-p\tau), \quad (7)$$

where $\nu = \sqrt{9/4 - m^2/H^2}$. As mentioned in the Introduction, the amplitude for the isocurvature mode $v_{\mathbf{p}}$ decays as $(-\tau)^{3/2-\nu}$ at late time $\tau \rightarrow 0$. If $m^2/H^2 > 9/4$, ν is imaginary, $v_{\mathbf{p}}$ has an additional fast oscillating factor, $\sim e^{\nu \ln(-k\tau/2)}$, even after the horizon exit. This suppresses its contribution. We will consider the case $0 \leq \nu < 3/2$, i.e. $9/4 \geq m^2/H^2 > 0$, in this paper.

The term that is responsible for the transformation from the isocurvature to curvature mode is (4). This introduces the “transfer vertex” (Fig. 1 (a)). The contribution from isocurvature to curvature correlation functions can therefore be computed according to the Feynman diagrams in Fig. 1 (b)(c). The term (5) is the leading

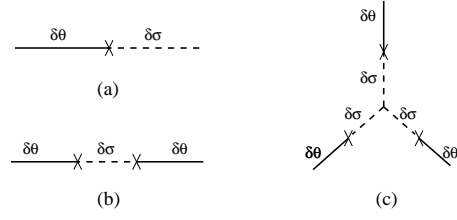


FIG. 1: Feynman diagrams for the transfer vertex (a), and the corrections from the isocurvature mode to the power spectrum (b) and bispectrum (c).

source for large non-Gaussianities, since all other cubic interactions in the expansion involve $\delta\theta$ which is in the slow-roll direction.

Bispectra. We compute the three-point correlation function $\langle \delta\theta^3 \rangle$. The bispectrum $\langle \zeta^3 \rangle$ is related to it through the usual time-delay relation $\zeta = -H\delta\theta/\dot{\theta}$.

The in-in formalism [4] gives

$$\langle \delta\theta^3 \rangle \equiv \langle 0 | \left[\bar{T} \exp \left(i \int_{t_0}^t d\tilde{t}' H_I(\tilde{t}') \right) \right] \delta\theta_I^3(t) \left[T \exp \left(-i \int_{t_0}^t dt' H_I(t') \right) \right] | 0 \rangle, \quad (8)$$

where t is the end of the inflation, and t_0 is the infinite past. The H_I is the interaction Hamiltonian,

$$H_I = \int d^3\mathbf{x} (\mathcal{H}_2^I + \mathcal{H}_3^I). \quad (9)$$

One can directly expand the exponentials in (8). For our purpose, the relevant terms are those involve four H_I 's. Each resulting quartic integral contains two “factors”. Each factor has a time-ordered integration but there is no cross time-ordering between the two. We call this form the “factorized form”. One can also rewrite all the integrands into one single time-ordered quartic integral,

$$\int_{t_0}^t dt_1 \int_{t_0}^{t_1} dt_2 \int_{t_0}^{t_2} dt_3 \int_{t_0}^{t_3} dt_4 \langle [H_I(t_4), [H_I(t_3), [H_I(t_2), [H_I(t_1), \delta\theta_I(t)^3]]]] \rangle. \quad (10)$$

We call this the “commutative form”. The Feynman diagram Fig. 1 (c) corresponds to replacing one of four H_I 's in (8) or (10) with H_3^I and the rest three with H_2^I . A straightforward exercise of Wick contraction leads to, for the factorized form,

$$\begin{aligned} & -12c_2^3 c_3 u_{p_1}^* u_{p_2} u_{p_3}(0) \\ & \times \text{Re} \left[\int_{-\infty}^0 d\tilde{\tau}_1 a^3 v_{p_1}^* u'_{p_1}(\tilde{\tau}_1) \int_{-\infty}^{\tilde{\tau}_1} d\tilde{\tau}_2 a^4 v_{p_1} v_{p_2} v_{p_3}(\tilde{\tau}_2) \right. \\ & \times \left. \int_{-\infty}^0 d\tau_1 a^3 v_{p_2}^* u'_{p_2}(\tau_1) \int_{-\infty}^{\tau_1} d\tau_2 a^3 v_{p_3}^* u'_{p_3}(\tau_2) \right] \\ & \times (2\pi)^3 \delta^3(\sum_i \mathbf{p}_i) + 9 \text{ other similar terms} \end{aligned}$$

+ 5 permutations of \mathbf{p}_i ; (11)

and for the commutator form,

$$\begin{aligned}
& 12c_2^3 c_3 u_{p_1}(0) u_{p_2}(0) u_{p_3}(0) \\
& \times \text{Re} \left[\int_{-\infty}^0 d\tau_1 \int_{-\infty}^{\tau_1} d\tau_2 \int_{-\infty}^{\tau_2} d\tau_3 \int_{-\infty}^{\tau_3} d\tau_4 \prod_{i=1}^4 (a^3(\tau_i)) \right. \\
& \times a(\tau_2) (u'_{p_1}(\tau_1) - c.c.) (v_{p_1}(\tau_1) v_{p_1}^*(\tau_2) - c.c.) \\
& \times (v_{p_3}(\tau_2) v_{p_3}^*(\tau_4) u_{p_3}^*(\tau_4) - c.c.) v_{p_2}(\tau_2) v_{p_2}^*(\tau_3) u_{p_2}^*(\tau_3) \left. \right] \\
& \times (2\pi)^3 \delta^3(\sum_i \mathbf{p}_i) + 2 \text{ other similar terms} \\
& + 5 \text{ permutations of } \mathbf{p}_i . \quad (12)
\end{aligned}$$

We write the argument τ_i only once if they are all the same in one integrand, and the prime denotes the derivative respective to the conformal time τ_i . The full details are presented in Ref. [6].

It is subtle to evaluate these integrals. Let us first look at the factorized form. In the UV limit, $\tau_i \rightarrow -\infty$, the integrands are fast oscillating. The convergence of the integration is achieved by slightly tilting the contour clockwise or counter-clockwise into the imaginary plane, $\tau_i \rightarrow -\infty(1 \pm i\epsilon)$. This corresponds to picking up the Bunch-Davies vacuum. In fact, if the integration is convergent at IR, $\tau \rightarrow 0$, it is numerically much more convenient to do a Wick rotation $\tau_i \rightarrow iz_i$ for the left factor and opposite for the right. The integration range for z_i is from $-\infty$ to 0. Now it is explicit that the integrand of each factor decays exponentially at UV. This is the case for $0 \leq \nu < 1/2$.

However, for $1/2 < \nu < 3/2$, using the asymptotic behavior of the mode functions, it is easy to see that each term in (11) is IR divergent. Physically, larger ν corresponds to smaller m for the isocurvature mode. So the mode decays slower. The conversion from isocurvature to curvature mode lasts longer after the horizon exit. As we will see, this causes slower convergence in the IR, but not divergence.

Let us look at this in the commutator form (12). Due to the subtraction of the complex conjugate in various terms, the integrand decreases faster in IR. For example, $u'_{p_1}(\tau_1)$ behaves as $(-\tau_1)$ as $\tau_1 \rightarrow 0$; but after subtracting off its complex conjugate, we have $(-\tau_1)^2$. The next two terms are slightly more complicated but similar. Since all these three terms are imaginary, $v_{p_2} v_{p_2}^* u_{p_2}^*$ in the 4th line must be imaginary to make the whole integration real. For $\tau_{2,3} \rightarrow 0$, the leading term of $v_{p_2} v_{p_2}^* u_{p_2}^*$ is real, so we need the subleading term in this limit. This also increases the IR convergence. Overall, it is not difficult to see that the IR convergence is achieved for all $0 \leq \nu < 3/2$. However, the Wick rotation no longer works in this form. The original integrands from the left and right factor have been multiplied together, so after Wick rotation, the exponential decay of some factors are cancelled by the exponential growth of the others.

To summarize, for $1/2 < \nu < 3/2$, the factorized form is well behaved in UV but encounters spurious divergence

in IR in the intermediate step. While the commutator form is well behaved in IR but the UV convergence becomes tricky [7]. Therefore we have proved that the whole integral has no divergence. In fact, to see both types of convergence at once, we can choose a cutoff τ_c in the middle, and make the whole expression take the factorized form in the UV, $\tau_i < \tau_c$, and commutator form in the IR, $\tau_i > \tau_c$ [6]. Numerical calculation for the full bispectrum shape still remains a challenge to us for $1/2 < \nu < 3/2$; but nonetheless we will see that this discussion becomes very useful in the squeezed limit.

Squeezed limit and shape ansatz. We now look at the squeezed limit, $p_3 \ll p_1 = p_2$. In this limit, simple analytical expressions of shapes are possible. This can also help us construct simple analytical ansatz for the full shape, to facilitate future data analyses.

Using the asymptotic behavior of the Hankel function, we can straightforwardly take the squeezed limit for Eqs. (11) and (12),

$$\frac{c_2^3 c_3}{H R^6} \frac{1}{p_1^{\frac{7}{2}-\nu} p_2 p_3^{\frac{3}{2}+\nu}} (s_{\text{fac}}(\nu) \text{ or } s_{\text{com}}(\nu)) , \quad (13)$$

where s_{fac} and s_{com} are p_i -independent numerical numbers, but involve complicated integrals [6]. The subscripts indicate the different forms that have been used. As we explained, it is crucial to pick an appropriate form to successfully carry out these numerical integrals. For $0 < \nu < 1/2$, s_{fac} is efficient. But as ν approaches $1/2$, cancellation of spurious IR divergence among different terms quickly breaks down the numerical calculation. So for $1/2 < \nu < 3/2$, we need s_{com} since this expression is explicitly convergent in IR. It turns out to be also convergent in UV even before regulating the UV oscillation. But for $\nu < 1/2$, the UV convergence of s_{com} becomes increasingly slower. The net result is presented in Fig. 2.

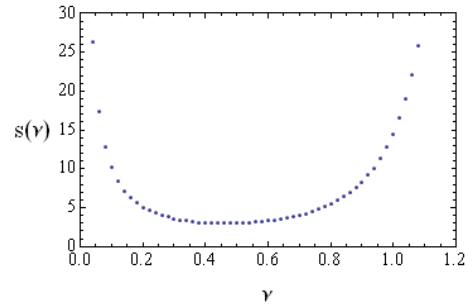


FIG. 2: The numerical coefficient $s(\nu)$ in the squeezed limit.

Some comments are in order, to explain the behavior of $s(\nu)$ near $\nu = 0$ and $\nu = 3/2$. We have approximated the asymptotic behavior of $H_\nu^{(1)}(-p_3 \tau_i)$ in the small p_3 limit as $-i(2^\nu \Gamma(\nu)/\pi)(-p_3 \tau_i)^{-\nu}$. For very small $\nu \sim 0$, this requires $p_3/p_1 \ll e^{-1/\nu}$. So p_3 needs to be increasingly small as $\nu \rightarrow 0$. Otherwise, if we fix a small p_3 , near

$\nu = 0$ we should instead use $i(2/\pi) \ln(-p_3 \tau_i)$ as a better approximation. Therefore the rising behavior in Fig. 2 near $\nu = 0$ does not mean that the non-Gaussianities are blowing-up, rather signals the change of the shape to

$$\sim \frac{\ln(p_3/p_1)}{p_1^{7/2} p_2 p_3^{3/2}}. \quad (14)$$

As $\nu \rightarrow 3/2$, $m \rightarrow 0$, the model is becoming a two-field single field model. This is beyond our validity region and other descriptions are necessary [9].

Combining (13) and (14), a good ansatz for the full shape can be taken as, up to an overall amplitude,

$$-\frac{(p_1 p_2 p_3)^{-3/2}}{(p_1 + p_2 + p_3)^{3/2}} N_\nu \left(\frac{p_1 p_2 p_3}{(p_1 + p_2 + p_3)^3} \right), \quad (15)$$

where N_ν is the Neumann Function. Depending on the value of ν , this ansatz can be further refined or simplified in terms of more elementary functions. We have compared this ansatz with the numerical results of the full shapes for $\nu = 0$ and $\nu = 0.2$, and found good match; for $1/2 < \nu < 3/2$, numerical calculation for the full shape is difficult, but at least their behavior in the squeezed limit match.

Note that in the squeezed limit, this one-parameter family of shapes goes as $p_3^{-3/2-\nu}$. This interpolates between the equilateral form, p_3^{-1} , and the local form, p_3^{-3} [10], so we call it the “intermediate form”. Two examples of the shape ansatz are shown in Fig. 3.

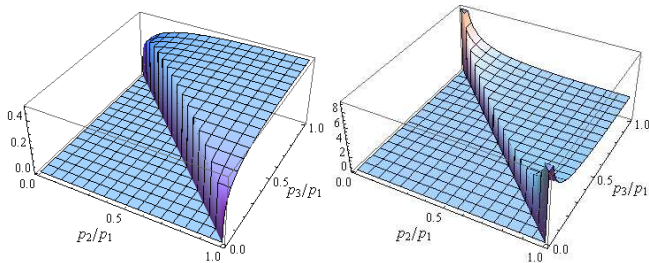


FIG. 3: Shapes of bispectra with intermediate form: 1) quasi-equilateral ($\nu = 0.2$), 2) quasi-local ($\nu = 1$). The amplitudes are normalized by a factor of $(p_1 p_2 p_3)^2$ to be dimensionless.

For comparison, we look at the three-point function of the isocurvature modes, $\langle \delta \sigma^3 \rangle$. Evaluate it after the horizon exit, we find that its amplitude is decaying and its shape goes as $p_3^{-2\nu}$ in the squeezed limit. So at least in this model, the shape of the correlation function is changed during the transfer. It is important to study this aspect in other multifield models.

Size of non-Gaussianities. The size f_{NL} of a bispectrum is defined by taking the equilateral limit [11],

$$\langle \zeta^3 \rangle \rightarrow \frac{9}{10} f_{NL} \frac{1}{p_1^6} P_\zeta^2 (2\pi)^7 \delta^3(\sum \mathbf{p}_i), \quad (16)$$

where P_ζ is the power spectrum. Using the relation $\zeta = -H \delta \theta / \dot{\theta}$ and $P_\zeta = H^4 / (4\pi^2 R^2 \dot{\theta}_0^2) \approx 2.3 \times 10^{-9}$, we get

$$f_{NL}^{\text{int}} = \alpha(\nu) \frac{1}{P_\zeta^{1/2}} \left(\frac{-V'''}{H} \right) \left(\frac{\dot{\theta}_0}{H} \right)^3. \quad (17)$$

We investigate the order of magnitude of each factor. The $\alpha(\nu)$ should be evaluated numerically, similar to $s(\nu)$, but now in the equilateral limit. For example it is $\mathcal{O}(1)$ and positive near $\nu = 0$. If we require that, in $V(\sigma)$, the quadratic term dominates over the cubic interaction for $\sigma \lesssim H$, so that we can trust the mode function, we need $|V'''|/H < (m_\sigma/H)^2 \sim \mathcal{O}(1)$. The perturbative method we used gives restriction on the size of $\dot{\theta}_0/H$ because this parameter determines the strength of the transfer vertex. For example, the correction to the power spectrum can be simply calculated using Fig. 1 (b), $\delta P_\zeta \sim (\dot{\theta}_0/H)^2 P_\zeta$, so for it to be perturbative we need $(\dot{\theta}_0/H)^2 \ll 1$. It is possible that the non-Gaussianity is larger if $\dot{\theta}_0/H \sim 1$, but to trust the perturbative results in this paper, $\dot{\theta}_0/H < \mathcal{O}(1)$. Overall we see that $|f_{NL}^{\text{int}}| < \mathcal{O}(10^4)$, and its sign is the opposite of V''' . It will be very interesting to constrain it using the current and future data [12]. It is also interesting to study what the natural values for V''' and $\dot{\theta}_0$ are from a more fundamental theory.

We thank B. Chen, A. Guth, Q.-G. Huang, and M. Li for helpful discussions and A. Frey for his participation in the early stage of this work. XC was supported by the US DOE under cooperative research agreement DEFG02-05ER41360. YW was supported by NSFC, NSERC and an IPP postdoctoral fellowship.

-
- [1] A. H. Guth, Phys. Rev. D **23**, 347 (1981). A. D. Linde, Phys. Lett. B **108**, 389 (1982). A. J. Albrecht and P. J. Steinhardt, Phys. Rev. Lett. **48**, 1220 (1982).
 - [2] E. J. Copeland, A. R. Liddle, D. H. Lyth, E. D. Stewart and D. Wands, Phys. Rev. D **49**, 6410 (1994). X. Chen, JCAP **0812**, 009 (2008).
 - [3] J. M. Maldacena, JHEP **0305**, 013 (2003). V. Acquaviva, N. Bartolo, S. Matarrese and A. Riotto, Nucl. Phys. B **667**, 119 (2003).
 - [4] For review, see S. Weinberg, Phys. Rev. D **72**, 043514 (2005).
 - [5] This requires $m_\sigma > \dot{\theta}_0$. The $\dot{\theta}_0$ will cause a displacement for the vev, we can redefine the σ and R so that $\sigma = 0$ is the effective minimum.
 - [6] X. Chen, Y. Wang, in preparation.
 - [7] The computational advantage of the factorized form has been noticed previously [8], while the commutator form has not.
 - [8] D. Seery, M. S. Sloth and F. Vernizzi, JCAP **0903**, 018 (2009). P. Adshead, R. Easther and E. A. Lim, arXiv:0904.4207 [hep-th]. X. Chen, B. Hu, M. x. Huang, G. Shiu and Y. Wang, JCAP **0908**, 008 (2009).
 - [9] M. Sasaki and E. D. Stewart, Prog. Theor. Phys. **95**, 71 (1996). D. H. Lyth and Y. Rodriguez, Phys.

- Rev. Lett. **95**, 121302 (2005) [arXiv:astro-ph/0504045].
G. I. Rigopoulos, E. P. S. Shellard and B. J. W. van Tent,
Phys. Rev. D **73**, 083521 (2006). D. Seery and J. E. Lid-
sey, JCAP **0509**, 011 (2005). F. Vernizzi and D. Wands,
JCAP **0605**, 019 (2006) D. Langlois, S. Renaux-Petel,
D. A. Steer and T. Tanaka, Phys. Rev. D **78**, 063523
(2008). F. Arroja, S. Mizuno and K. Koyama, JCAP
0808, 015 (2008).
- [10] D. Babich, P. Creminelli and M. Zaldarriaga, JCAP
0408, 009 (2004). X. Chen, M. x. Huang, S. Kachru and
G. Shiu, JCAP **0701**, 002 (2007).
- [11] E. Komatsu *et al.* [WMAP Collaboration], Astrophys. J.
Suppl. **180**, 330 (2009).
- [12] E. Komatsu *et al.*, arXiv:0902.4759 [astro-ph.CO].